(41)

Measuring Precision of Three-Dimensional Landmark Data

BRIAN D. CORNER,[1,2] SUBHASH LELE,[3] and JOAN T. RICHTSMEIER[1]

[1] *Department of Cell Biology and Anatomy, The Johns Hopkins University School of Medicine, Baltimore, MD, 21205*
[2] *Present address: US Army Natick Research, Development & Engineering Center, Natick, MA, 01760-5020*
[3] *Department of Biostatistics, The Johns Hopkins University, School of Hygiene and Public Health, Baltimore, MD, 21205*

ABSTRACT: Technological advances have led to an increase in collection of three-dimensional coordinate landmark data for morphometric analysis. Unlike more conventional distance measurements, three-dimensional data have not had the benefit of close scrutiny. In this study we examine measurement error separately along X, Y, and Z coordinate axes. A formal statistical model is developed to test for precision along the three axes and applied in a data collection experiment using the Polhemus 3Space digitizer. Our results indicate that measurement error is not disproportionately greater along any of the three principle axes. Although this was expected for our data collection instrument, we feel that our model will be of most use when three-dimensional landmark coordinates are collected from three-dimensional reconstructions produced by various imaging modalities. We conclude with suggestions on how to increase precision.

KEY WORDS: measurement error, digitizer, 3D image data

In the past few years technology for the collection of three-dimensional data has become more accessible, and the number of morphometric techniques for the quantitative analysis of these data has grown (e.g., Siegel and Benson 1982; Cheverud et al. 1983; Goodall 1991; Lele 1991; Lele and Richtsmeier 1991, 1992; Rohlf and Slice 1990; Rohlf and Bookstein 1990). Three-dimensional (3D) coordinates of biological landmarks provide a valid model of the relative position of landmarks on a form although certain types of information (e.g., surface contours) are not part of the model (Figure 1). The benefit of recording a biological form using 3D coordinates of landmarks lies in the maintenance of geometric integrity of the form under study and the ability to calculate a large set of linear distances from the locations of biological landmarks.

Unlike distance measurements, 3D coordinate data has not had the benefit of close scrutiny. Thus, biases and sources of error in this type of data are not well known. Knowledge of error is critical to data reliability and plays directly into appropriate interpretation of results. This study was

Journal of Quantitative Anthropology 3: 347–359, 1992.

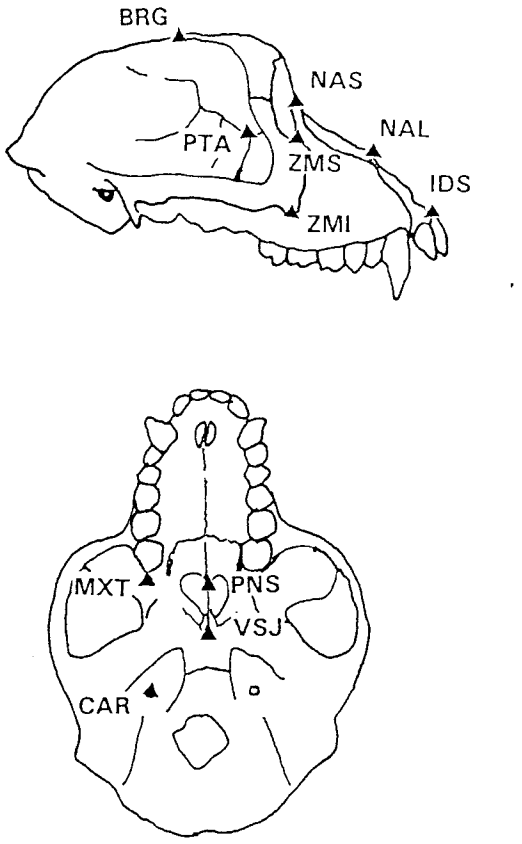

Fig. 1. Lateral (A) and basicranial (B) views of a drawing of a *Macaca fascicularis* skull showing landmark position. Landmark abbreviations are given in Table I.

prompted by our own use of 3D coordinate data sets collected using various techniques and by the growing number of studies that utilize 3D coordinate data.

This is a study of *precision*. Precision is the average absolute difference between repeated measures of the same individual (Kohn and Cheverud 1992). Lack of precision results in variability among repeated measures of the same individual. Variability among repeated measures occurs due to observer error in locating landmarks and instrument error in identifying landmark coordinates.

The study of *repeatability*, in contrast to precision, involves the repeated measure of several individuals and includes biological variability as a contributor to measurement error. Repeatability is the precision of a particular measurement relative to the biological differences among individuals contrasted in any given study. It is measured as the proportion of

total variance due to differences between individuals using a repeated measures analysis of variance design (Kohn and Cheverud 1992; Falconer 1981).

Inclusion of more than one data collection episode for multiple individuals requires that X, Y, Z coordinate values be translated and rotated when forms are compared. Precision and repeatability of 3D coordinate data are routinely measured by superimposing data sets so that a particular parameter is minimized. This rigid body motion does not change the relative location of landmarks positioned on each form, but does change the coordinate values for the landmarks thereby concealing the separate contribution of error along the three major axes. Our goal is to present a model that enables the calculation of precision for the location of 3D landmarks separately along each of the three major axes. Since rigid body motion prevents accurate evaluation of precision measured along the three principal axes we consider a single individual and do not examine repeatability.

The design presented here is not meant to replace existing repeatability (e.g., Falconer 1981; Kohn and Cheverud 1992) or validation models (Vannier et al. 1991; Kohn and Cheverud 1992) that allow the researcher to quantify the degree of error from various sources (e.g., the measuring or imaging device, the researcher, morphological variability within a population). We suggest that repeatability and/or validation models should be applied to determine the contribution of various sources of measurement error. When a large proportion of measurement error is attributed to the collection device and the researcher, and the researcher has reason to believe that a measuring device is disproportionately prone to error along a particular axis, our model for the study of precision should then be applied.

We study precision in data collected using the Polhemus 3Space digitizer which has been subjected to previous validation and measurement error studies (Hildebolt and Vannier 1988; Richtsmeier and Danahey, unpublished data). The models used in those studies did not enable the calculation of separate precision estimates for the X, Y, and Z axes. We elected this measurement device as an appropriate test instrument for our model because of our extensive experience with the instrument. Given our familiarity with the 3Space digitizer and previous validation studies of this instrument (Hildebolt and Vannier 1988), we expect that error in locating a biological landmark is evenly distributed along the three axes.

MATERIALS AND METHODS

The data collection system consists of a tabletop model 3Space digitizer interfaced with a COMPAQ 286 Deskpro personal computer (PC). The

system is easy to use. When an object is positioned on the table in a preferred orientation, the tip of a hand held stylus is placed on the landmark to be recorded. A foot- or keypad is pressed to record the landmark's coordinates. The digitizer uses an electromagnetic field generated from a unit in the digitizer table to determine the position of sensors built into the stylus. When all the landmarks have been located on a specimen, the coordinates are saved in ASCII format to a file on the PC. Stored in this format, the data files can be easily imported into any software for analysis or display.

For our study of observer measurement error, the following data gathering experiment was designed. Two observers (BDC and JTR) collected data from 11 landmarks (Table I, Figure 1) from the face and cranium of a single skull, a subadult male *Macaca fascicularis*. The skull was digitized twenty times by each observer. Data were collected twice daily, with approximately six hours separating the daily digitizations, until each sample of 20 digitizations was complete.

TABLE I
List of the eleven landmarks digitized. Abbreviations in brackets are used in the text.

(1)	Nasion [NAS]
(2)	Nasale [NAL]
(3)	R. Zygomaxillare inferior [ZMI]
(4)	R. Zygomaxillare superior [ZMS]
(5)	Intradentale superior [IDS]
(6)	Posterior nasal spine: Vomer-Palatine intersection [PNS]
(7)	R. Maxillary Tuberosity: Maxillary-Palatine junction [MXT]
(8)	Vomer-Sphenoid junction [VSJ]
(9)	R. Pterion Anterior: Zygo-Spheno-Frontal junction [PTA]
(10)	Bregma [BRG]
(11)	R. Carotid Canal: center of canal [CAR]

Importantly, the specimen was fixed to the digitizer table using plasticine (Figure 2). Lack of movement of the object between digitizations removes the necessity of rotating and translating the various data sets in calculating measurement error enabling the estimation of error along each of the three major axes. This design is comparable to repeatedly collecting the same landmarks from a single image (e.g., computed tomographic, ultra-sound, magnetic resonance) of a biological form. Having controlled for different object orientation, we can estimate the precision around each landmark due solely to the researcher's ability to consistently locate a landmark on a single form using a particular measuring device.

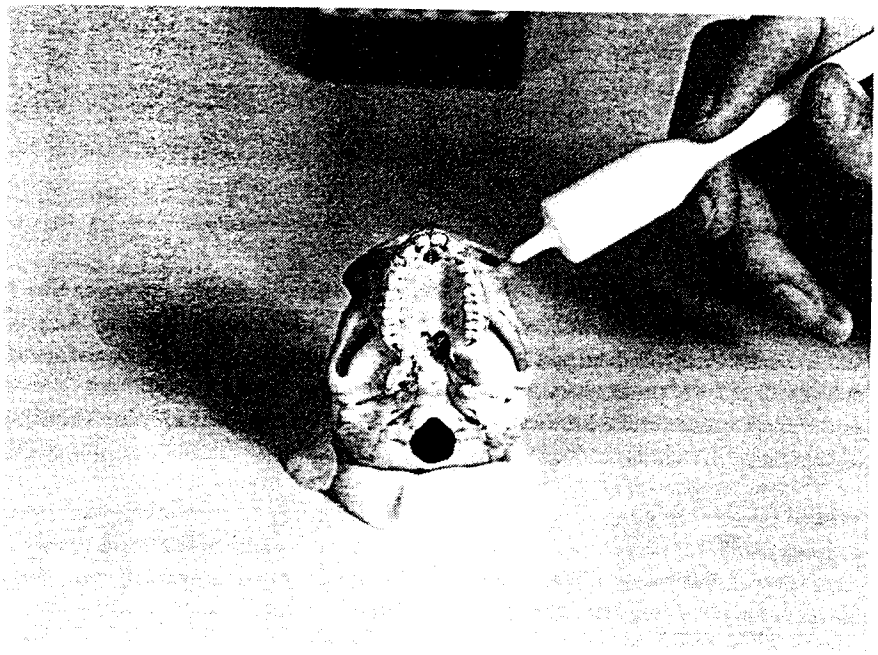

Fig. 2. Skull fixed on the 3Space digitizer table top for data collection.

STATISTICAL MODEL AND ESTIMATION

Let $\mathbf{M}$ be the (11×3) matrix of true (but unknown) landmark coordinates for 11 biological landmarks on the stationary skull. When one measures the skull n times, one gets n nonidentical matrices: $\mathbf{M}_1, \mathbf{M}_2, \ldots, \mathbf{M}_n$. They are not identical to each other due to observer and machine error. Our model as presented does not enable us to separate observer from machine error.

We used the following to model the variability in $\mathbf{M}_1, \mathbf{M}_2, \ldots, \mathbf{M}_n$:

$$\mathbf{M}_i = \mathbf{M} + \mathbf{E}_i \qquad i = 1, 2, \ldots, n$$

where:

$$M = \begin{vmatrix} M_{1x} & M_{1y} & M_{1z} \\ M_{2x} & M_{2y} & M_{2z} \\ M_{3x} & M_{3y} & M_{3z} \\ \cdot & \cdot & \cdot \\ \cdot & \cdot & \cdot \\ M_{11x} & M_{11y} & M_{11z} \end{vmatrix}$$

and E_i represents a (11 × 3) matrix of the 3D error at each landmark:

$$E_i = \begin{vmatrix} e_{1x} & e_{1y} & e_{1z} \\ e_{2x} & e_{2y} & e_{2z} \\ e_{3x} & e_{3y} & e_{3z} \\ \cdot & \cdot & \cdot \\ \cdot & \cdot & \cdot \\ e_{11x} & e_{11y} & e_{11z} \end{vmatrix}$$

The $\mathbf{E}_i$s are assumed to be independent identically distributed matrix valued Gaussian random variables with mean zero and variance-covariance matrix $\mathbf{\Sigma}$. $\mathbf{\Sigma}$ is a positive definite matrix of dimension 33 × 33 and represents the random measurement error due to observer and machine factors. $\mathbf{\Sigma}$ can be written in a partitioned form:

$$\mathbf{\Sigma} = \begin{vmatrix} \Sigma_{XX} & \Sigma_{XY} & \Sigma_{XZ} \\ \Sigma_{XY} & \Sigma_{YY} & \Sigma_{YZ} \\ \Sigma_{XZ} & \Sigma_{YZ} & \Sigma_{ZZ} \end{vmatrix}$$

where each entry is a 11 × 11 submatrix. Let us consider one of these submatrices, $\mathbf{\Sigma}_{XX}$, more closely:

$$\mathbf{\Sigma}_{XX} = \begin{vmatrix} \alpha_{1x1x} & \alpha_{1x2x} & \alpha_{1x3x} & \cdot & \cdot & \alpha_{1x11x} \\ \alpha_{2x1x} & \alpha_{2x2x} & \alpha_{2x3x} & \cdot & \cdot & \alpha_{2x11x} \\ \alpha_{3x1x} & \alpha_{3x2x} & \alpha_{3x3x} & \cdot & \cdot & \alpha_{3x11x} \\ \cdot & \cdot & \cdot & \cdot & \cdot & \cdot \\ \cdot & \cdot & \cdot & \cdot & \cdot & \cdot \\ \cdot & \cdot & \cdot & \cdot & \cdot & \cdot \\ \alpha_{11x1x} & \alpha_{11x2x} & & \cdot & \cdot & \alpha_{11x11x} \end{vmatrix}$$

The first element in column 1 is the variance along the X axis at landmark 1 over the 20 data collection episodes. The second element in column 1 is the covariance along the X axis for landmarks 1 and 2 over the twenty data collection episodes. The remainder of the entries and those for the other submatrices can be interpreted in similar fashion.

From standard multivariate analysis (e.g., Mardia et al. 1979), we calculate the maximum likelihood estimators of the mean, $\mathbf{M}$, and variance matrix, $\mathbf{\Sigma}$, using the following:

$$\hat{M} = \frac{1}{n} \sum_{i=1}^{n} M_i$$

and

$$\hat{\Sigma} + \frac{1}{n} \sum_{i=1}^{n} (M_i^c - \hat{M}^c)(M_i^c - \hat{M}^c)^T$$

where M_i^c and $\hat{M}^c$ are written in vector format:

$$M_i^c = (M_{1X,i}, M_{2X,i}, \ldots, M_{11X,i}, M_{1Y,i}, M_{2Y,i}, \ldots M_{11Y,i}, M_{1Z,i}, M_{2Z,i}, \ldots M_{11Z,i})^T$$

and

$$\hat{M}^c = (\hat{M}_{1X}, \hat{M}_{2X}, \ldots, \hat{M}_{11X}, \hat{M}_{1Y}, \hat{M}_{2Y}, \ldots \hat{M}_{11Y}, \hat{M}_{1Z}, \hat{M}_{2Z}, \ldots \hat{M}_{11Z})^T$$

RESULTS

Each observer shows a high consistency in locating the 11 landmarks. This is clearly seen in Table II, which provides the standard deviation of each coordinate for the eleven landmarks digitized. The maximum standard deviation for both observers along any of the three axes is approximately 0.45 mm. Most of the values of Table II, however, are considerably lower than this extreme. The consistently low variation in coordinate values across the three dimensions indicates that no single direction is particularly prone to error for any of the landmarks considered. These results support our expectation of equal distribution of error along the three axes.

Table II also demonstrates that observer 2 did somewhat better at consistently locating landmarks throughout the experiment. However both observers produced data with error evenly distributed among the three axes. Our model was not developed for the purpose of calculating inter-observer error and we do not feel that application of our model to the study of inter-observer error would improve the precision of the data. Previously published models can be used to calculate inter-observer error from more typical data sets when such quantities are desired.

TABLE II

Standard deviations (mm) of landmark coordinates from data gathered in Experiment 1. Landmark abbreviations are from Table I.

	Standard Deviation (mm) of Landmark Coordinates					
	Observer 1			Observer 2		
LMK	*X*	*Y*	*Z*	*X*	*Y*	*Z*
NAS	0.249	0.379	0.248	0.173	0.256	0.195
NAL	0.248	0.451	0.378	0.361	0.229	0.304
ZMI	0.163	0.208	0.338	0.154	0.143	0.336
ZMS	0.246	0.385	0.417	0.199	0.280	0.446
IDS	0.297	0.395	0.259	0.287	0.170	0.205
PNS	0.201	0.281	0.270	0.228	0.350	0.373
MXT	0.211	0.180	0.289	0.300	0.157	0.446
VSJ	0.226	0.146	0.253	0.294	0.166	0.383
PTA	0.224	0.258	0.343	0.196	0.216	0.212
BRG	0.165	0.197	0.204	0.194	0.219	0.330
CAR	0.200	0.234	0.239	0.335	0.201	0.278

DISCUSSION

Based on the results of our data gathering experiment, our recommendations for minimizing measurement error using a similar 3D digitizer include: (1) familiarity of the researcher with the digitizer; and (2) thorough knowledge by the researcher of landmark location and variability in landmark expression between specimens. Although we did not study the impact of population variability on measurement error, we recognize its importance. An appreciation for the variation in landmark expression in the population being digitized is critical to the collection of accurate data. Adequate training and familiarity with the sample and the digitizer can minimize many of the potential sources of error.

When landmark data are collected but linear distances computed from the landmark locations are used in analysis, measurement error is intrinsic to the landmarks and is independent of the linear distance computed from those landmarks. Consequently the impact that observer measurement error has on the reliability of distance data varies with the distance. That is, if you have a consistently low measurement error as we do, the proportion of error is greater over small distances than it is over larger distances. To illustrate this point, the coefficient of variation for linear distances calculated from the landmarks is given in Table III. As expected, the coefficient of variation for the smaller distances is much greater than that for larger distances. The imprecision that can be tolerated in a study varies with the measures being used.

We purposefully included several different landmark types in our choice of landmarks. The intersections of osseous sutures, extremal points along a suture or bone, and foramen are three landmark types included in our set of landmarks (Table I). No obvious pattern of measurement error was found among the different types of landmarks. However, distances that include posterior nasal spine (PNS), zygomaxillare superior (ZMS) and nasale (NAL), tend to have higher standard deviations (Table III). These landmarks are all extreme ends of sutures located on an osseous edge. We suggest that researchers be sensitive to the possible higher amount of measurement error associated with this type of landmark, especially when the landmarks are endpoints of measures that span short distances.

For all but the smallest linear distances reported here ($<$ 1 cm) we feel that the calculated standard deviations represent acceptable degrees of observer measurement error. If observer measurement error in 3D coordinate data is a concern however, the error can be easily minimized by taking repeated observations from a fixed object. An entire skull can be digitized several times, or landmarks that are particularly close to one another can be recorded an additional number of times (e.g. a total of 4 times) while other landmarks can be recorded only once. If the number of

TABLE III

Mean distance (n = 20), standard deviation, and coefficient of variation for Euclidean distances between all possible pair of landmarks. For each observer, the linear distances are presented in ascending order according to the length of the linear distances. All measurement are in centimeters. Landmark abbreviations are from Table I. The coefficient of variation (CV) is expressed as a percent.

Observer 1				Observer 2			
Landmarks	Mean Dist.	SD	CV[1]	Landmarks	Mean Dist.	SD	CV
PNS-VSJ	0.724	0.0414	5.708	PNS-VSJ	0.71	0.0389	5.469
PNS-MXT	0.944	0.0295	3.119	PNS-MXT	0.951	0.0297	3.13
MXT-VSJ	1.284	0.0301	2.348	MXT-VSJ	1.324	0.0396	2.995
ZMI-MXT	1.374	0.019	1.384	ZMI-MXT	1.387	0.0331	2.386
NAL-ZMS	1.534	0.0232	1.516	NAL-ZMS	1.562	0.0355	2.278
ZMI-PTA	1.553	0.0281	1.811	ZMI-PTA	1.595	0.0272	1.707
ZMI-ZMS	1.695	0.0296	1.749	NAL-IDS	1.615	0.054	3.346
NAL-IDS	1.703	0.0295	1.736	ZMI-ZMS	1.668	0.0484	2.902
ZMS-PTA	1.819	0.0269	1.48	ZMS-PTA	1.777	0.055	3.099
MXT-PTA	1.882	0.0248	1.319	NAS-ZMS	1.884	0.0553	2.939
NAS-ZMS	1.89	0.0198	1.05	MXT-PTA	1.943	0.0401	2.066
NAS-NAL	1.973	0.0259	1.316	NAS-NAL	1.973	0.0283	1.434
VSJ-PTA	1.979	0.0313	1.584	VSJ-PTA	2.006	0.0316	1.579
ZMI-PNS	2.015	0.0296	1.471	ZMI-PNS	2.026	0.0342	1.688
MXT-CAR	2.138	0.0338	1.581	VSJ-CAR	2.066	0.0342	1.656
VSJ-CAR	2.141	0.0189	0.886	MXT-CAR	2.125	0.0351	1.654
PNS-PTA	2.158	0.0349	1.62	PNS-PTA	2.168	0.0354	1.636
ZMI-VSJ	2.332	0.0269	1.152	ZMS-PTA	2.291	0.0449	1.961
ZMS-PNS	2.333	0.022	0.944	ZMS-MXT	2.35	0.033	1.404
NAL-MXT	2.353	0.0268	0.799	ZMI-VSJ	2.361	0.0265	1.123
ZMS-MXT	2.382	0.0174	0.731	PNS-CAR	2.419	0.033	1.367
PNS-CAR	2.498	0.026	1.043	ZMS-VSJ	2.541	0.0553	2.178
ZMS-VSJ	2.583	0.0183	0.711	ZMS-IDS	2.599	0.0356	1.369
ZMS-IDS	2.63	0.0183	0.697	NAS-PTA	2.7	0.0288	1.068
NAL-PTA	2.715	0.0312	1.149	PTA-CAR	2.764	0.0228	0.825
PTA-CAR	2.781	0.0253	0.913	NAL-ZMI	2.949	0.0399	1.353
NAL-ZMI	2.963	0.042	1.419	NAL-PNS	2.965	0.0341	1.149
NAL-PNS	2.983	0.0205	0.69	NAS-VSJ	3.054	0.0287	0.94
NAS-VSJ	3.061	0.0271	0.888	ZMI-CAR	3.111	0.0336	1.079
ZMI-CAR	3.109	0.0361	1.164	NAS-PNS	3.114	0.0323	1.038
NAS-PNS	3.126	0.0205	0.658	NAL-PTA	3.261	0.0374	1.456
NAL-PTA	3.265	0.0322	0.986	ZMI-IDS	3.29	0.0363	1.104
ZMI-IDS	3.322	0.0376	1.133	NAL-MXT	3.33	0.048	1.443
NAL-VSJ	3.362	0.0253	0.752	NAL-VSJ	3.34	0.321	0.963
NAS-ZMI	3.399	0.035	0.899	NAS-ZMI	3.402	0.246	0.723
IDS-PNS	3.526	0.0268	0.76	IDS-PNS	3.52	0.0292	0.831
NAS-MXT	3.603	0.021	0.585	NAS-IDS	3.574	0.0436	1.222
NAS-IDS	3.659	0.0282	0.772	NAS-MXT	3.616	0.0311	0.861
IDS-MXT	3.716	0.0326	0.878	IDS-MXT	3.684	0.0301	0.808

Table III (continued)

Observer 1				Observer 2			
Landmarks	Mean Dist.	SD	CV[1]	Landmarks	Mean Dist.	SD	CV
IDS-VSJ	4.138	0.026	0.628	ZMS-CAR	4.075	0.0486	1.192
ZMS-CAR	4.172	0.0252	0.605	IDS-VSJ	4.112	0.0364	0.885
PTA-BRG	4.217	0.0213	0.505	IDS-PTA	4.23	0.0455	1.076
IDS-PTA	4.262	0.034	0.797	PTA-BRG	4.231	0.0542	1.281
VSJ-BRG	4.303	0.0435	1.011	VSJ-BRG	4.305	0.031	0.72
NAS-BRG	4.371	0.0266	0.608	NAS-BRG	4.388	0.0584	1.332
BRG-CAR	4.662	0.0235	0.505	BRG-CAR	4.61	0.0372	0.808
NAS-CAR	4.928	0.0317	0.643	NAS-CAR	4.852	0.0361	0.744
PNS-BRG	4.987	0.0362	0.727	PNS-BRG	4.973	0.0402	0.81
NAL-CAR	5.292	0.0309	0.584	NAL-CAR	5.213	0.0423	0.811
MXT-BRG	5.305	0.0281	0.531	ZMS-BRG	5.317	0.0549	1.033
ZMS-BRG	5.33	0.0244	0.459	MXT-BRG	5.358	0.04	0.76
ZMI-BRG	5.706	0.0253	0.445	ZMI-BRG	5.75	0.0493	0.858
IDS-CAR	5.84	0.0269	0.461	IDS-CAR	5.782	0.0386	0.668
NAL-BRG	6.143	0.0281	0.457	NAL-BRG	6.151	0.0598	0.972
IDS-BRG	7.63	0.0239	0.313	IDS-BRG	7.582	0.0469	0.619

[1] CV = (standard deviation/mean distance) * 100

digitizations of landmarks is not uniform throughout the object, fixing the object is necessary so that mean coordinates from the repeated observations can be easily computed without the use of superimposition that involves computational effort and potential error due to varying orientation.

Determining the number of repeated observations per skull depends primarily on three factors: (1) the distance between landmarks; (2) landmark type and definition; and (3) the desired level of observer measurement error minimization. The distance between landmarks is determined by the size of the object, and the distribution of the landmarks on the object. Smaller objects tend to have landmarks that are closer together. If we use the skull as an example, certain anatomical regions (e.g. the cranial base) have more closely spaced landmarks than others (e.g. the neurocranium). If proximity is the only criterion for determining the number of repeated observations, digitizing all landmarks twice and those on the cranial base three or four times is suggested. Further consideration must be given to the landmark type (sutural intersection versus extremal points). Easily recognized and located landmarks need not be digitized repeatedly while those that are more ambiguously defined and physically difficult to reach require additional digitizations. The amount of time spent digitizing each specimen is critical when many landmarks are being

recorded from a large sample. In this case we suggest that problematic landmarks be repeatedly digitized (3 to 4 times). The cost of spending additional time digitizing must be weighed against improvement in data precision.

As stated previously, we had no suspicion of disproportionate error along the three major axes in data collected using the 3Space digitizer. However, there are data sets collected from other sources which we feel could be disproportionately prone to error along a single axis. For example, when computer tomographic (CT) images are produced, the unit of measure for two axes in the horizontal plane (X and Y) is the same and is defined according to pixel size. The scale of the third axis (Z) however is determined by the thickness of the slice. As the gantry moves over the patient, its location relative to the patient is highly controlled and referred to as table position. In conventional CT scanning the thinnest slices are 1 or 2 mm. thick. When 3D coordinates are collected from slice images (see for example Richtsmeier et al. 1990), a landmark is located in the X and Y plane according to pixel column and row, while the Z coordinate is assigned according to table position. This means that the X and Y coordinates of a landmark located on a slice will be defined in terms of pixels (which are often sub-millimeter in size) while the Z coordinate can only be estimated according to the table position (measured in 1 to 2 mm increments) of the slice within which the landmark is located. The spatial resolution of the Z coordinate of landmark location cannot be less than the slice thickness. Our next goal is to apply the model presented here to data collected from CT scans of a skull that we have also measured using the 3Space digitizer. The model that we have presented which requires repeated measures from a fixed object is well suited to the analysis of data collected repeatedly from a single image.

When landmark data are collected from a 3D reconstruction of an image, the three axes are defined according to the same scale, but the algorithms used to reconstruct the image, (the slice thickness and whether the slices are produced contiguously or in an overlapping fashion) may result in disproportionate levels of precision along the major axes. We have found in attempting to locate landmarks on 3D reconstructions (Kontis and Richtsmeier, unpublished data) that landmark type and consistency in orienting the reconstruction while locating the landmark have a profound effect on measurement error. For example, landmarks located on an osseous edge can only be recorded when the electronic cursor senses bone density. Once the cursor moves beyond the boundary of the reconstruction, a coordinate location cannot be recorded. This means that a landmark of this type located on a reconstructed image of a skull will not be on the osseous edge but will consistently be displaced towards the center of the skull. Error for this landmark collected form an image will be constrained in a particular direction.

The level of imprecision that can be tolerated in any particular study will vary with the magnitude of the contrast being made (Kohn and Cheverud 1992). For example, less stringent constraints on error levels are required for measurements used for a comparison of subadult macaque skulls with those of adult macaques than is required for comparing two samples of subadult individuals. We suggest that data collected from a single individual and analyzed using our model is acceptable if error does not exceed 3% of the distance calculated between landmarks. Once error exceeds 5%, it is unacceptable.

We stress that the model we have proposed should be used in conjunction with one that can partition error among various potential sources. Our model is intended for use when the researcher has reason to believe that error is disproportionately distributed among the major axes. We suggest that this may be the case for data collected from certain types of 3D images.

ACKNOWLEDGEMENTS

This research was supported in part by a grant from the Whitaker Foundation and a JHUIPRGP award.

REFERENCES CITED

Cheverud, J. M., Lewis, L. J., Bachrach, W., and Lew, W. B. 1983 The measurement of form and variation in form: an application of three-dimensional quantitative morphology by finite-element methods. Am. J. Phys. Anthropol. 62: 151—165.

Falconer, D. S. 1981 Introduction of Quantitative Genetics. Second edition, Longman, New York. 340 pp.

Goodall, C. 1991 Procrustes methods in the statistical analysis of shape. J. Roy. Statist. Soc. Ser. B 53, 285—339.

Hildebolt, C. F. and Vannier, M. W. 1988 3-D measurement accuracy of skull surface landmarks. Am. J. Phys. Anthropol. 76(4): 497—504.

Kohn, L. A. and Cheverud, J. M. 1992 Issues in evaluating repeatability of an imaging system for use in anthropometry. Proceedings of the Electronic imaging of the Human body working group, Crew System Ergonomics Information Analysis Center, Dayton, OH.

Lele, S. 1991 Some comments on coordinate free and scale invariant methods in morphometrics. Amer. J. Phys. Anthropol. 85: 407—418.

Lele, S. and Richtsmeier, J. T. 1990 Statistical models in morphometrics: are they realistic? Syst. Zool. 39(1): 60—69.

Lele, S. and Richtsmeier, J. T. 1991 Euclidean distance matrix analysis: a coordinate free approach for comparing biological shapes using landmark data. Amer. J. Phys. Anthropol. 86(3): 415—428.

Lele, S. and Richtsmeier, J. T. 1992 On comparing biological shapes: detection of influential landmarks. Amer. J. Phys. Anthropol. 87(1): 49—66.

Mardia, K. V., Kent, T., and Bibby, J. M. 1979 Multivariate Analysis. New York: Academic Press.

Richtsmeier, J. T., Grausz, H. M., Morris, G. R., Marsh, J. L., and Vannier, M. W. 1991 Growth of the cranial base in craniosynostosis. Cleft Palate Craniofac. J. (28)1: 55—67.

Rohlf, J. and Bookstein, F. L. (eds.) 1990 Proceedings of the Michigan morphometrics workshop. Special Publication Number 2, The University of Michigan Museum of Zoology, 380 pp.

Rohlf, J. and Slice, D. 1990 Extensions of the Procrustes methods for the optimal superimposition of landmarks. Syst. Zool. 39(1): 40—59.

Siegel, A. F. and Benson, R. H. 1982 A robust comparison of biological shapes. Biometrics 38: 341—350.

Vannier, M. W., Brunsden, B. S., Hildebolt, C. F., Falk, D., Cheverud, J. M., Figiel, G. S., Perman, W. H., Kohn, L. A., Robb, R. A., Yoffie, R. L., and Bresina, S. J. 1991 Brain surface cortical sulcal lengths: quantification with three-dimensional MR imaging. Radiology 180: 479—484.